

INTERACTION NOTES

Note 333

February 1978

TIME DOMAIN ANALYSIS OF MULTICONDUCTOR TRANSMISSION
LINES WITH BRANCHES IN INHOMOGENEOUS MEDIA

Ashok K. Agrawal, Howard M. Fowles,
Larry D. Scott and Larry T. Simpson

Mission Research Corporation
5601 Domingo Road, N. E.
Post Office Box 8693
Albuquerque, New Mexico 87108

ABSTRACT

An effective method for computing the time domain response of lossless multiconductor transmission lines with branches in a cross-sectionally inhomogeneous dielectric media is presented. Lines of this type are characterized by multiple propagation modes having different velocities. The theory of wave propagation on lossless multiconductor transmission lines with inhomogeneous dielectrics is used to obtain the modal amplitudes on the uniform sections of the line. The scattering matrix for the junction is used to compute the transmitted and reflected waves in the different branches at the junction. Each mode arriving at the junction excites multiple modes in all branches. The method described in this paper identifies all propagation modes in all branches of the line and leads to the direct physical interpretation of the results. The method is general and can be applied to either partially or completely nondegenerate cases. Experimental results for a six-conductor transmission line having a single branch are found to be in good agreement with the results computed using the described method.

CONTENTS

Section		Page
I	INTRODUCTION	5
II	DETERMINATION OF MODAL AMPLITUDES ON A UNIFORM SECTION OF LINE	7
III	SCATTERING MATRIX OF THE JUNCTION	13
IV	EXPERIMENTAL RESULTS	19
V	CONCLUDING REMARKS	31
	REFERENCES	32

ILLUSTRATIONS

Figure		Page
1	A Three-Wire Line Over a Ground Plane	10
2	A Multiconductor Transmission Line With a Branch	14
3	Five-Wire Cable (Over a Ground Plane) Configuration	21
4	Input Waveform Used to Drive the Wire in the Cable.	24
5	Voltage Waveform At the Load End of Wire 1 of Tube 2, with Wire 4 of Tube 1 Driven.	24
6	Voltage Waveform At the Load End of Wire 2 of Tube 2, with Wire 4 of Tube 1 Driven.	24
7	Voltage Waveform At the Load End of Wire 3 of Tube 2, with Wire 4 of Tube 1 Driven.	25
8	Voltage Waveform At the Load End of Wire 4 of Tube 3, with Wire 4 of Tube 1 Driven.	25
9	Voltage Waveform At the Load End of Wire 5 of Tube 3, with Wire 4 of Tube 1 Driven.	25
10	Voltage Waveform At the Load End of Wire 1 of Tube 1, with Wire 1 of Tube 2 Driven.	26
11	Voltage Waveform At the Load End of Wire 2 of Tube 1, with Wire 1 of Tube 2 Driven.	26
12	Voltage Waveform At the Load End of Wire 3 of Tube 1, with Wire 1 of Tube 2 Driven.	26
13	Voltage Waveform At the Load End of Wire 4 of Tube 1, with Wire 1 of Tube 2 Driven.	27
14	Voltage Waveform At the Load End of Wire 5 of Tube 1, with Wire 1 of Tube 2 Driven.	27
15	Voltage Waveform At the Load End of Wire 4 of Tube 3, with Wire 1 of Tube 2 Driven.	27

ILLUSTRATIONS (continued)

Figure		Page
16	Voltage Waveform At the Load End of Wire 5 of Tube 3, with Wire 1 of Tube 2 Driven.	28
17	Voltage Waveform At the Load End of Wire 1 of Tube 1, with Wire 4 of Tube 3 Driven.	28
18	Voltage Waveform At the Load End of Wire 2 of Tube 1, with Wire 4 of Tube 3 Driven.	28
19	Voltage Waveform At the Load End of Wire 3 of Tube 1, with Wire 4 of Tube 3 Driven.	29
20	Voltage Waveform At the Load End of Wire 4 of Tube 1, with Wire 4 of Tube 3 Driven.	29
21	Voltage Waveform At the Load End of Wire 5 of Tube 1, with Wire 4 of Tube 3 Driven.	29
22	Voltage Waveform At the Load End of Wire 1 of Tube 2, with Wire 4 of Tube 3 Driven.	30
23	Voltage Waveform At the Load End of Wire 2 of Tube 2, with Wire 4 of Tube 3 Driven.	30
24	Voltage Waveform At the Load End of Wire 3 of Tube 2, with Wire 4 of Tube 3 Driven.	30

SECTION I INTRODUCTION

Electronic subsystems on aircraft, missiles and ground electronic systems are generally connected by closely coupled multiconductor cables. These multiconductor cables are generally made of conductors with different insulating materials resulting in a cross-sectionally inhomogeneous media. Such cables often have branches where some of the conductors of the cable branch and/or some other conductors may join the cable. Determination of the transient response of such cables illuminated by an electromagnetic pulse (EMP) from nuclear detonations is becoming of increasing importance (ref. 1).

The analysis of uniform multiconductor transmission lines have been reported by several investigators both in the frequency and the time domain (refs. 2 through 12). The propagation modes for multiconductor transmission lines with inhomogeneous dielectrics are discussed in reference 4. The analysis of multiconductor transmission line networks in the frequency domain is given in reference 5. The present paper describes the theory of wave propagation on lossless multiconductor transmission lines with branches in cross-sectionally inhomogeneous media in the time domain.

The method of analysis described in this paper identifies separately all the propagation modes in all the branches of the multiconductor line. While many individual parts of this problem appear elsewhere (refs. 4 and 5), this paper presents a complete time domain analysis of a multiconductor transmission line with branches. In general, for a uniform multiconductor transmission line (N conductors plus a ground reference) in a cross-sectionally inhomogeneous media, there will be N propagation modes each having a different velocity. Degeneracies may occur among the velocities because of symmetry. These modes are separated in time as they travel along the line. Each mode arriving at a junction excites multiple modes in the

branches at that junction. The scattering matrix for the junction (refs. 5, 6 and 16) is used to compute the transmitted and reflected waves in the different branches at the junction. At any mismatched termination or junction each reflected mode excites N modes in a $N+1$ conductor line. Thus, the number of modes are multiplied for each reflection.

The method described in this paper can be applied to a partially degenerate case where some modes have the same propagation velocities. In this case, the modes having the same velocities arrive at a junction or termination at the same time.

SECTION II
 DETERMINATION OF MODAL AMPLITUDES
 ON A UNIFORM SECTION OF LINE

Consider a lossless line formed by N conductors, plus a reference conductor (ground). The line is assumed to be uniform along its length (z coordinate), but with arbitrary cross-section. In general, the dielectric surrounding the line is inhomogeneous (e.g., cable made of insulated conductors having different geometries and dielectric materials).

In the presence of materials of different dielectric constants, the propagation can not strictly be TEM. However, for low frequencies propagation may be considered "quasi-TEM" (refs. 4 and 13), and the analysis can proceed from the generalized telegrapher's equations. These equations for the lossless case are (refs. 3 and 14),

$$\frac{\partial}{\partial z} [V_n(z,t)] = -[L'_{nm}] \frac{\partial}{\partial t} [I_m(z,t)] \quad (1)$$

$$\frac{\partial}{\partial z} [I_n(z,t)] = -[C'_{nm}] \frac{\partial}{\partial t} [V_m(z,t)] \quad (2)$$

with $n = 1, 2, \dots, N$
 $m = 1, 2, \dots, N$

Where V_m and I_m represent the voltage with respect to the reference conductor and current on the m th conductor, respectively, as a function of distance z along the line at time, t. $[L'_{nm}]$ and $[C'_{nm}]$ are respectively per-unit-length coefficients of inductance and capacitance matrices of $N \times N$ size. The diagonal elements are self and the off-diagonal elements are mutual quantities. Both $[L'_{nm}]$ and $[C'_{nm}]$ are real, symmetric and dominant. The



elements of the capacitance matrix $[C'_{nm}]$ and inductance matrix $[L'_{nm}]$ are further characterized by the following properties (ref. 15):

$$\begin{aligned}
 L'_{nm} &\geq 0 \text{ for all } n \text{ and } m \\
 C'_{nn} &\geq 0 \text{ for all } n \\
 C'_{nm} &\leq 0 \text{ for all } n \neq m \\
 \sum_{m=1}^N C'_{nm} &\geq 0 \text{ for all } n \\
 \sum_{n=1}^N C'_{nm} &\geq 0 \text{ for all } m
 \end{aligned} \tag{3}$$

The voltage and current vectors in Eq. (1) and (2) can be written as (ref. 4)

$$[V_n(z,t)] = [V_n] f(z-vt) \tag{4}$$

$$[I_n(z,t)] = [I_n] f(z-vt) \tag{5}$$

where $[V_n]$ and $[I_n]$ are the constant vectors. From Eqs. (1), (2), (4) and (5) the eigenvalue equation for $[V_n]$ can be written as

$$[L'_{nm}][C'_{nm}][V_n]_i = 1/v_i^2 [V_n]_i \tag{6}$$

where $1/v_i^2$ is an eigenvalue of the matrix $[L'_{nm}][C'_{nm}]$, and $[V_n]_i$ the associated voltage eigenvector. In the case of inhomogeneous dielectrics there will in general be N distinct eigenvalues. Associated with the eigenvalues $1/v_i^2$, $i=1, \dots, N$, there are also current eigenvectors $[I_n]_i$. The $[I_n]_i$ are the eigenvectors of the adjoint matrix $[C'_{nm}][L'_{nm}]$ and have the

same eigenvalues $1/v_i^2$ (ref. 4). The eigenvalue equation for this case can be written as

$$[C'_{nm}][L'_{nm}][I_n]_i = 1/v_i^2 [I_n]_i \quad (7)$$

The analysis can proceed either with the voltage or the current eigenvectors. The voltage or current eigenvectors are computed from Eqs. (6) or (7). The per-unit-length inductance matrix $[L'_{nm}]$ and capacitance matrix $[C'_{nm}]$ can be measured experimentally using the methods described in references 17 or 18. The determination of $[L'_{nm}]$ and $[C'_{nm}]$ analytically is generally a difficult problem. However, numerical approximations can be employed to determine $[L'_{nm}]$ and $[C'_{nm}]$ (refs. 19 and 20). Thus, the eigenvalues and the voltage or current eigenvectors of the transmission line can be obtained by solving the eigenvalue, Eq. (6) or (7).

It can be shown that in order for the modes to represent unattenuated traveling waves, the velocities must be real (i.e., the eigenvalues $1/v_i^2$ must be real and positive)(ref. 4). The v_i 's represent the velocities of N propagating modes.

Since the modes of propagation are orthogonal to each other, the eigenvectors form a set of linearly independent vectors, an arbitrary vector $[E_n]$ can be represented as a sum of voltage eigenvectors in the form (ref. 4)

$$[E_n] = [V_{nm}][A_m] \quad (8)$$

where $[A_m]$ is a vector.

Let a wave traveling in the forward direction be characterized at some point in space and time by the voltage vector $[V_{f_n}(z,t)]$ which can be expressed in terms of the voltage eigenvectors as

$$[V_{f_n}(z,t)] = [V_{nm}][A_m(t)] \quad (9)$$

where the vector $[A_m(t)]$ is unknown.

Consider a line of length ℓ connected to arbitrary terminal networks at each end (Figure 1), and excited at the end $z=0$. The different modes propagate at different velocities, so that the knowledge of $[V_{f_n}(z,t)]$ at one time is not sufficient to obtain $[V_{f_n}(z,t)]$ at other times. Also, knowing $[V_{f_n}(z,t)]$ at one point on the line (e.g., driving end) is not sufficient to obtain the $[V_{f_n}(z,t)]$ at any other point on the line because of the different propagating velocities of the modes. So, $[V_{f_n}(z,t)]$ at $z=0$ must be decomposed into eigenvectors

$$[V_{f_n}(0,t)] = [V_{nm}] [A_n(t)]$$

or
$$V_{f_n}(0,t) = \sum_{m=1}^N V_{nm} A_m(t) \quad (10)$$

The forward traveling voltage vector at any point $z=\ell$ on the line may be determined as readily.

Define the transit time for each mode as

$$\tau_i = \ell/v_i, \quad i=1, 2, \dots, N.$$

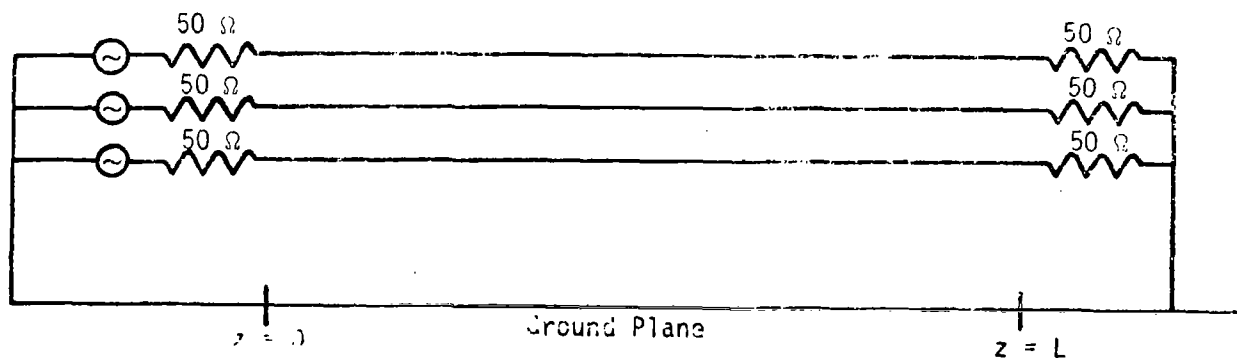


Figure 1. A Three-Wire Line Over a Ground Plane

The desired voltage vector $[V_{f_n}(z,t)]$ at $z = \ell$ is obtained from $[V_{f_n}(0,t)]$ by adding eigenvectors at the appropriate transit time after leaving the point $z = 0$

$$V_{f_n}(\ell,t) = \sum_{m=1}^M V_{nm} A_m(t-\tau_m) \quad (11)$$

where $V_{f_n}(\ell,t)$ is the n^{th} component of the vector $[V_{f_n}(\ell,t)]$. The voltage $[V_{f_n}(\ell,t)]$ will have N components due to N modes. Thus, $V_{f_n}(\ell,t)$ can be represented as $N \times N$ matrix whose rows are the components of the elements of $[V_{f_n}(\ell,t)]$. This is illustrated by considering an example of a four conductor line. For this case, Eq. (11) can be written as

$$\begin{bmatrix} V_{f_1}(\ell,t) \\ V_{f_2}(\ell,t) \\ V_{f_3}(\ell,t) \end{bmatrix} = \begin{bmatrix} V_{11} & V_{12} & V_{13} \\ V_{21} & V_{22} & V_{23} \\ V_{31} & V_{32} & V_{33} \end{bmatrix} \begin{bmatrix} A_1(t-\tau_1) \\ A_2(t-\tau_2) \\ A_3(t-\tau_3) \end{bmatrix} \quad (12)$$

or

$$V_{f_1}(\ell,t) = V_{11} \cdot A_1(t-\tau_1) + V_{12} \cdot A_2(t-\tau_2) + V_{13} \cdot A_3(t-\tau_3) . \quad (13)$$

The other two components can be expressed similarly.

Note that in Eq. (13), the voltage wave incident at any point $z=\ell$ on the conductors has three components. These voltages represent the modal amplitudes of the different modes. The voltage wave, traveling in the forward direction at $z = 0$ can be obtained from the following relation.

$$[V_{f_n}(0,t)] = [Z_{c_{nm}}] [Z_{c_{nm}} + Z_{s_{nm}}]^{-1} [V_{s_n}(0,t)] \quad (14)$$

where $[Z_{c_{nm}}]$ is the characteristic impedance matrix of the line, $[Z_{s_{nm}}]$ the

termination impedance matrix at the driven end and $[V_{s_n}(0,t)]$ the source voltage vector at $z = 0$. Thus, from Eq.(13) and Eq.(14) the modal amplitudes at any point on the line can be obtained. The waves on a lossless line travel unattenuated. At any discontinuity or load the voltage or current can be obtained using the reflection and transmission coefficients. For a uniform section of the line (Figure 1) the voltage vector at the load is given by the following relation

$$[V_{L_n}(t)]_m = 2[Z_{L_{nm}}][Z_{L_{nm}} + Z_{C_{nm}}]^{-1} [V_{f_n}(\ell,t)]_m \quad (15)$$

where $[V_{L_n}(t)]_m$ is the load voltage vector for the m^{th} mode, $[Z_{L_{nm}}]$ and $[Z_{C_{nm}}]$ are the load and characteristic impedance matrices, respectively, and $[V_{f_n}(\ell,t)]_m$ is the incident voltage vector at the load for the m^{th} mode.

At any junction, the reflected and transmitted waves in different branches are obtained by using the scattering matrix of the junction. In the next section, the junction characteristics will be described.

SECTION III
SCATTERING MATRIX OF THE JUNCTION

For distributed circuits, the reflected and incident waves at a junction can be related by a scattering matrix (reference 16). The procedures for evaluating the scattering matrix for transmission line junctions are discussed in detail in reference 5. In this section these procedures will be described briefly and the scattering matrix for a branched multiconductor line will be evaluated. The experimental results will be given in Section IV.

For the junction shown in Figure 2, the incident and reflected voltages for a lossless case are related by the following relation

$$\begin{bmatrix} [V_n^{(re)}]_1 \\ [V_n^{(re)}]_2 \\ [V_n^{(re)}]_3 \end{bmatrix} = [S_{nm}] \begin{bmatrix} [V_n^{(i)}]_1 \\ [V_n^{(i)}]_2 \\ [V_n^{(i)}]_3 \end{bmatrix} \quad (16)$$

where $[V_n^{(re)}]_i$, $i=1,2,3$ are the reflected voltage vectors for the various tubes meeting at the junction and $[V_n^{(i)}]_i$, $i=1,2,3$ are the incident voltage vectors for the various tubes meeting at the junction. The size of the vectors $[V_n^{(re)}]_i$ and $[V_n^{(i)}]_i$ is equal to the number of the conductors in the tube. The components of these vectors represent the voltages on the individual conductors. $[S_{nm}]$, in Eq. (16), is the scattering matrix of the junction which is considered lossless. For the junction shown in Figure 2, the scattering matrix is 10×10 in size.

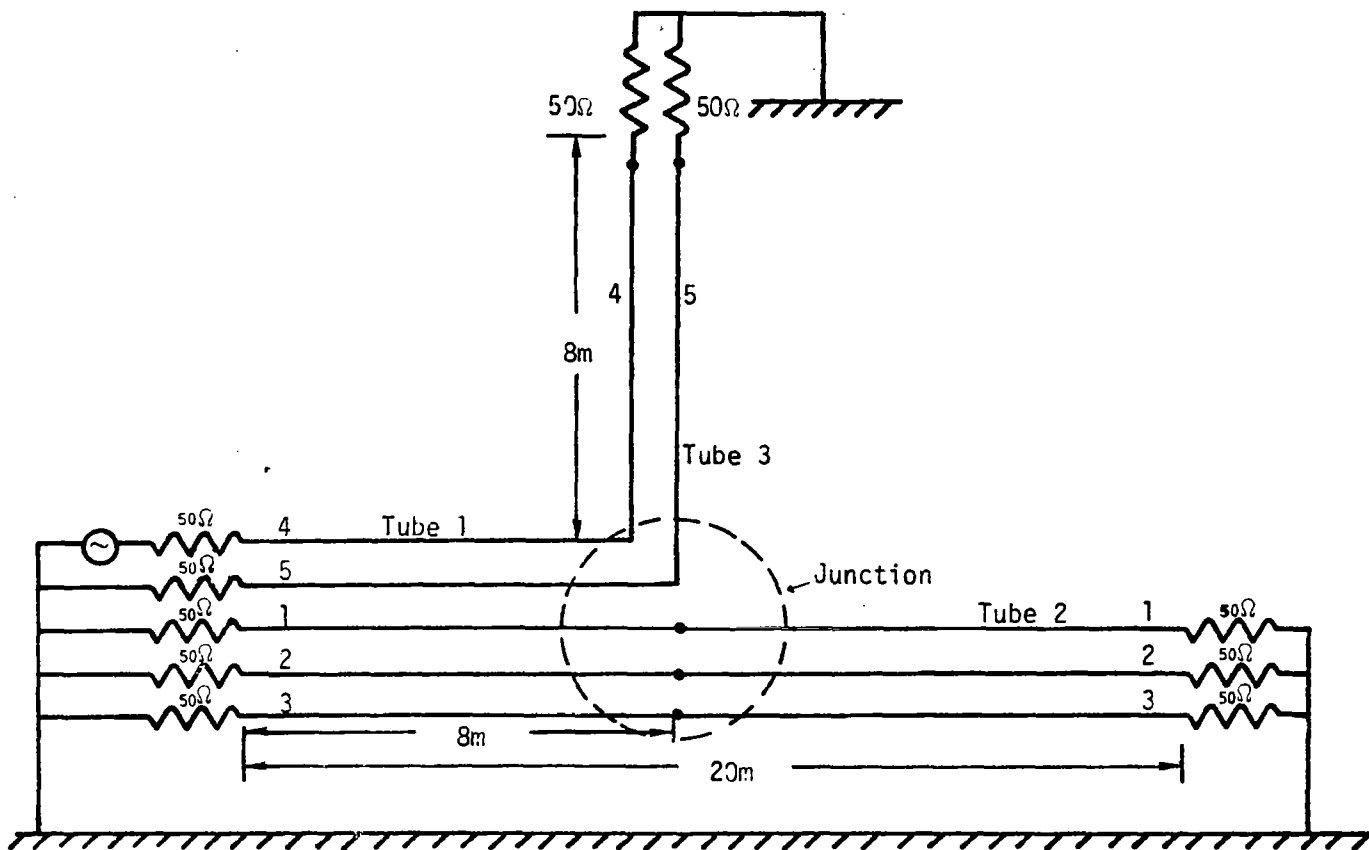


Figure 2. A Multiconductor Transmission Line With a Branch

At the junction where there are several tubes interconnected to one another, the Kirchhoff's current law and the Kirchhoff's voltage law have to be enforced in order to evaluate the scattering matrix of the junction.

Kirchhoff's current law states that the sum of the current flowing into a node is zero. For the case where n_1 -th wire of tube 1 is connected to the n_2 -th wire of tube 2 and to the n_k -th wire of tube k, etc., then

$$(I_{n1})_1 + (I_{n2})_2 + \dots + (I_{nk})_k = 0 \quad (17)$$

where the subscripts on the parentheses denote the tube number and the subscripts on I denote the wire number in the tube. Eq. (17) can be put into matrix form, i.e.,

$$\begin{matrix}
 \text{Tube 1} & & \text{Tube 2} & & & & \text{Tube k} \\
 [0 & 0 \dots 1 \dots 0] & | & 0 & 0 \dots 1 \dots 0 & | & \dots & | & 0 & 0 \dots 1 \dots
 \end{matrix}
 \begin{bmatrix}
 [I_n]_1 \\
 [I_n]_2 \\
 \vdots \\
 [I_n]_k
 \end{bmatrix}
 = [0] \quad (18)$$

In Eq.(18), all elements in the left matrix are zero unless they correspond to the conductors which are connected at the node. For N_c connections within the junction, there are N_c equations similar to Eq.(18), and we can define the junction connection matrix $[C_{I_{nm}}]$ so that

$$[C_{I_{nm}}]
 \begin{bmatrix}
 [I_n]_1 \\
 [I_n]_2 \\
 \vdots \\
 [I_n]_k
 \end{bmatrix}
 = [0_n] \quad (19)$$

where $[C_{I_{nm}}]$ is a $N_c \times M_j$ matrix, and M_j is the total number of conductors entering the junction.

Kirchhoff's voltage law, for the case of simple connections, requires all voltages associated with each conductor to be the same at the same node. Thus, for the above example, we have

$$\begin{aligned}
(v_{n1})_1 - (v_{n2})_2 &= 0 \\
(v_{n2})_2 - \dots &= 0 \\
\dots\dots\dots & \\
\dots\dots - (v_{nk})_k &= 0
\end{aligned} \tag{20}$$

For a consistent set of connections, there are $M_j - N_c$ equations. The above equation can be easily written in matrix form. Let us denote the corresponding matrix as $[C_{V_{nm}}]$ such that

$$[C_{V_{nm}}] \begin{bmatrix} [V_n]_1 \\ [V_n]_2 \\ \vdots \\ [V_n]_k \end{bmatrix} = [0_n] \tag{21}$$

where $[C_{V_{nm}}]$ is a $(M_j - N_c) \times M_j$ matrix.

At the junction the total current and voltage is the sum of the two components, i.e., the incident and reflected components (ref: 16),

$$[V_n] = [V_n^{(i)}] + [V_n^{(re)}] \tag{22}$$

$$[I_n] = [I_n^{(i)}] - [I_n^{(re)}] \tag{23}$$

Using Eqs. (19), (21), (22) and (23) the relation between the reflected and incident voltage components at the junction can be written as

$$\begin{bmatrix} [V_n^{(re)}]_1 \\ [V_n^{(re)}]_2 \\ \vdots \\ [V_n^{(re)}]_k \end{bmatrix} = \begin{bmatrix} [-C_{V_{nm}}] \\ [C_{I_{nm}}][Y_{C_{nm}}] \end{bmatrix}^{-1} \begin{bmatrix} [C_{V_{nm}}] \\ [C_{I_{nm}}][Y_{C_{nm}}] \end{bmatrix} \begin{bmatrix} [V_n^{(i)}]_1 \\ [V_n^{(i)}]_2 \\ \vdots \\ [V_n^{(i)}]_k \end{bmatrix} \quad (24)$$

From Eq. (24) the voltage scattering matrix is

$$[S_{nm}] = \begin{bmatrix} [-C_{V_{nm}}] \\ [C_{I_{nm}}][Y_{C_{nm}}] \end{bmatrix}^{-1} \begin{bmatrix} [C_{V_{nm}}] \\ [C_{I_{nm}}][Y_{C_{nm}}] \end{bmatrix} \quad (25)$$

where $[Y_{C_{nm}}]$ is the characteristic admittance matrix of the junction. $[Y_{C_{nm}}]$ can be obtained from the characteristic impedance matrix $[Z_{C_{nm}}]$. The matrix $[Z_{C_{nm}}]$ contains all the matrices of all branches involved at the junction. For the junction shown in Figure 2 it can be expressed as

$$[Z_{C_{nm}}] = \begin{bmatrix} [Z_{C_{nm}1}] & [0_{nm}] & [0_{nm}] \\ [0_{nm}] & [Z_{C_{nm}2}] & [0_{nm}] \\ [0_{nm}] & [0_{nm}] & [Z_{C_{nm}3}] \end{bmatrix} \quad (26)$$

The characteristic impedance matrices $[Z_{C_{nm}b}]$ for each branch can be obtained by methods described in reference 21.

The voltage modal amplitudes incident at the junction are computed using the method described in Section II. From Eq. (16), the voltage amplitudes reflected in different branches at the junction are obtained. The method of analysis described in Section II, is used to compute the voltage waves arriving at the loads of the different branches using the transmitted waves in the branch at the junction as excitations.

As mentioned earlier, multiple modes are excited on a multiconductor transmission line in inhomogeneous media. Each mode reflected from the junction or the load in turn excites multiple modes in the branch. Using the analysis described in this paper, all of the modes excited at subsequent times may be calculated. Thus, by following the straightforward step-by-step procedure, the response of the line in the time domain can be obtained. It should be noted, that when multiple reflections from the junction and the loads are considered, the number of modes traveling on the line become large. In some practical cases, the weaker modes having small amplitudes can be neglected for multiple reflections in determining the total response.

SECTION IV EXPERIMENTAL RESULTS

To substantiate the calculational methods discussed in this paper, a five-wire cable (over a ground plane) with a two-wire branch was constructed and tested. Wires insulated with solid polyethylene, neoprene, rubber, foam polyethylene and semisolid polyethylene were used for the cable construction. The configuration is shown in Figure 2. The cable was supported with styro-foam blocks above an aluminum ground plane. The cross-sectional configuration of a five-wire line is shown in Figure 3. Wires 4 and 5 branch and at a 90° angle at 8 meters distance and wires 1, 2 and 3 continue with the same relative cross-sectional configuration. The radii of the conductors, (r_i), and the distance between the centers of the wires, (d_{ij}) are as follows:

$r_1 = 0.108$ cm	$d_{12} = 0.70$ cm	$d_{24} = 0.68$ cm
$r_2 = 0.062$ cm	$d_{13} = 0.54$ cm	$d_{25} = 1.02$ cm
$r_3 = 0.062$ cm	$d_{14} = 0.69$ cm	$d_{34} = 0.93$ cm
$r_4 = 0.111$ cm	$d_{15} = 0.60$ cm	$d_{35} = 0.49$ cm
$r_5 = 0.0125$ cm	$d_{23} = 1.16$ cm	$d_{45} = 0.59$ cm

The experimentally measured per-unit-length inductance and capacitance matrices for the five-wire line, three-wire line and two-wire line sections are, respectively,

$$[L'_{nm}]_{\text{meas}} = \begin{bmatrix} 0.902 & 0.477 & 0.540 & 0.485 & 0.513 \\ 0.477 & 0.951 & 0.384 & 0.486 & 0.424 \\ 0.540 & 0.384 & 1.006 & 0.424 & 0.534 \\ 0.485 & 0.486 & 0.424 & 0.850 & 0.557 \\ 0.513 & 0.424 & 0.534 & 0.557 & 1.116 \end{bmatrix} \mu\text{H/m};$$

$$[C'_{nm}]_{\text{meas}} = \begin{bmatrix} 52.555 & -16.125 & -17.761 & -8.895 & -5.632 \\ -16.125 & 42.145 & -2.319 & -15.357 & -1.426 \\ -17.761 & -2.319 & 35.779 & -3.146 & -6.841 \\ -8.895 & -15.357 & -3.146 & 41.772 & -9.705 \\ -5.632 & -1.426 & -6.841 & -9.705 & 25.355 \end{bmatrix} \text{pF/m}$$

(5-wire Line)

$$[L'_{nm}]_{\text{meas}} = \begin{bmatrix} 0.884 & 0.484 & 0.535 \\ 0.484 & 0.939 & 0.379 \\ 0.535 & 0.379 & 0.992 \end{bmatrix} \mu\text{H/m}; [C'_{nm}] = \begin{bmatrix} 46.48 & -20.909 & -20.553 \\ -20.909 & 33.834 & -4.152 \\ -20.553 & -4.152 & 31.099 \end{bmatrix} \text{pF/m}$$

(3-wire Line)

$$[L'_{nm}]_{\text{meas}} = \begin{bmatrix} 0.829 & 0.533 \\ 0.533 & 1.101 \end{bmatrix} \mu\text{H/m}; [C'_{nm}] = \begin{bmatrix} 26.746 & -14.684 \\ -14.684 & 20.052 \end{bmatrix} \text{pF/m}$$

(2-wire Line)

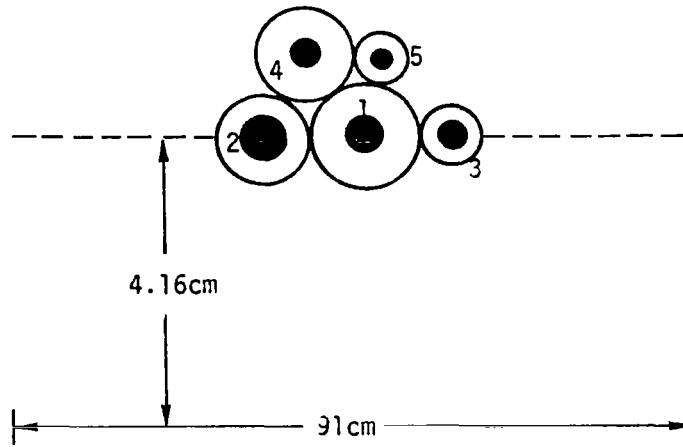


Figure 3. Five-Wire Cable (Over a Ground Plane) Configuration

For the junction in Figure 2, the connection matrix is

$$[C_{I_{nm}}] = \begin{bmatrix} 1 & 0 & 0 & 0 & 0 & 1 & 0 & 0 & 0 & 0 \\ 0 & 1 & 0 & 0 & 0 & 0 & 1 & 0 & 0 & 0 \\ 0 & 0 & 1 & 0 & 0 & 0 & 0 & 1 & 0 & 0 \\ 0 & 0 & 0 & 1 & 0 & 0 & 0 & 0 & 1 & 0 \\ 0 & 0 & 0 & 0 & 1 & 0 & 0 & 0 & 0 & 1 \end{bmatrix} \quad (27)$$


$$[C_{V_{nm}}] = \begin{bmatrix} 1 & 0 & 0 & 0 & 0 & -1 & 0 & 0 & 0 & 0 \\ 0 & 1 & 0 & 0 & 0 & 0 & -1 & 0 & 0 & 0 \\ 0 & 0 & 1 & 0 & 0 & 0 & 0 & -1 & 0 & 0 \\ 0 & 0 & 0 & 1 & 0 & 0 & 0 & 0 & -1 & 0 \\ 0 & 0 & 0 & 0 & 1 & 0 & 0 & 0 & 0 & -1 \end{bmatrix} \quad (28)$$

The experimentally measured characteristic impedance matrix of the junction as defined in Eq. (26) and the scattering matrix of the junction computed from Eq. (25) are shown in Table 1.

Table 1. Characteristic Impedance and Scattering Matrices

$$[Z_{c_{nm}}] = \begin{bmatrix} 223.073 & 138.964 & 150.885 & 138.278 & 145.372 & 0 & 0 & 0 & 0 & 0 & 0 \\ 138.964 & 229.164 & 115.579 & 140.97 & 125.528 & 0 & 0 & 0 & 0 & 0 & 0 \\ 150.885 & 115.579 & 247.95 & 123.761 & 149.056 & 0 & 0 & 0 & 0 & 0 & 0 \\ 138.278 & 140.97 & 123.761 & 225.051 & 155.647 & 0 & 0 & 0 & 0 & 0 & 0 \\ 145.372 & 125.528 & 149.056 & 155.647 & 295.409 & 0 & 0 & 0 & 0 & 0 & 0 \\ 0 & 0 & 0 & 0 & 0 & 232.419 & 148.328 & 159.83 & 0 & 0 & 0 \\ 0 & 0 & 0 & 0 & 0 & 148.382 & 237.879 & 121.279 & 0 & 0 & 0 \\ 0 & 0 & 0 & 0 & 0 & 159.83 & 121.279 & 258.32 & 0 & 0 & 0 \\ 0 & 0 & 0 & 0 & 0 & 0 & 0 & 0 & 227.59 & 156.939 & 156.939 \\ 0 & 0 & 0 & 0 & 0 & 0 & 0 & 0 & 156.939 & 302.948 & 302.948 \end{bmatrix}$$

$$[S_{nm}] = \begin{bmatrix} .06775 & .07147 & .05039 & -.25665 & -.15288 & .93224 & -.07147 & -.05039 & .25665 & .15288 \\ .07334 & .07258 & .03348 & -.30059 & -.09414 & -.07334 & .92741 & -.03348 & .300592 & .09414 \\ .06688 & .05086 & .05896 & -.19562 & -.18852 & -.06688 & -.05086 & .94103 & .19527 & .18852 \\ -.16315 & -.20131 & -.09141 & .10854 & .05009 & .16315 & .20131 & .09141 & .89145 & -.05009 \\ -.17621 & -.11906 & -.17501 & .08759 & .07822 & .17621 & .11906 & .17501 & -.08759 & .92177 \\ 1.06776 & .07147 & .05039 & -.25665 & -.15288 & -.06775 & -.07147 & -.05039 & .25665 & .15288 \\ .07334 & 1.07259 & .03348 & -.30059 & -.09414 & -.07334 & -.07258 & -.03348 & .30059 & .09414 \\ .06688 & .05086 & 1.05896 & -.19562 & -.18852 & -.06688 & -.05086 & -.05896 & .19562 & .18852 \\ -.16315 & -.20131 & -.09141 & 1.10855 & .05009 & .16315 & .20131 & .09141 & -.10854 & -.05009 \\ -.17621 & -.11906 & -.17501 & .08759 & 1.07822 & .176218 & .11906 & .17501 & -.08759 & -.07822 \end{bmatrix}$$



To obtain the time domain response of the cable of Figure 2, one wire of a tube is driven with a fast risetime step function (ps) from a 50-ohm source and all remaining ends of wires terminated in 50-ohm resistive loads. The voltage responses on each wire in all tubes were recorded using a high impedance voltage probe and a 200 MHz oscilloscope. To demonstrate the consistency of the analysis, one wire was driven in each of the tubes and the voltage pulses were recorded at the ends of the other tubes.

Figure 4 shows the input step function used to drive the wires as viewed on the 200 MHz oscilloscope. Figures 5 through 9 show the comparison of voltage waveforms recorded at the load ends of tubes 2 and 3, when wire 4 of tube 1 is driven, with the waveforms computed using the analysis described in this paper. One set of computed waveforms are analytically filtered to reflect the 200 MHz bandwidth of the oscilloscope for a more direct comparison between the measured response and the predicted response. The unfiltered waveforms clearly show the times of arrival of different modes. Figures 10 through 16 show the comparison of voltage waveforms recorded at the load ends of tubes 1 and 3, when wire 1 of tube 2 is driven, with the waveforms computed. Figures 17 through 24 show the comparison of voltage waveforms recorded at the load ends of tubes 1 and 2, when wire 4 of tube 3 is driven with the waveforms computed.

The computed waveforms in Figures 5 through 24 have been obtained by assuming an ideal step function as the input. The driving pulse has an apparent rise time of approximately 2 ns as seen in Figure 4 as recorded with the 200 MHz bandwidth oscilloscope used for all measurements. The comparison in Figures 5 through 24 shows that the predicted waveforms agree very closely with the measured waveforms. Note that, in Figures 5 through 9, the predicted waveforms, after being filtered to simulate the 200 MHz bandwidth of the oscilloscope, agree remarkably with the measured waveforms. The predicted amplitudes of different modes, and their times of arrival, compare closely with those of the measured data.

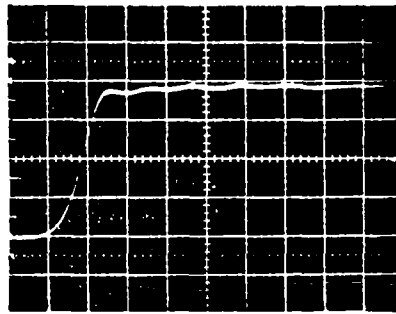


Figure 4. Input Waveform Used to Drive the Wire in the Cable.
Vertical Scale is 1.0 V/div; Horizontal Scale is 2 ns/div.

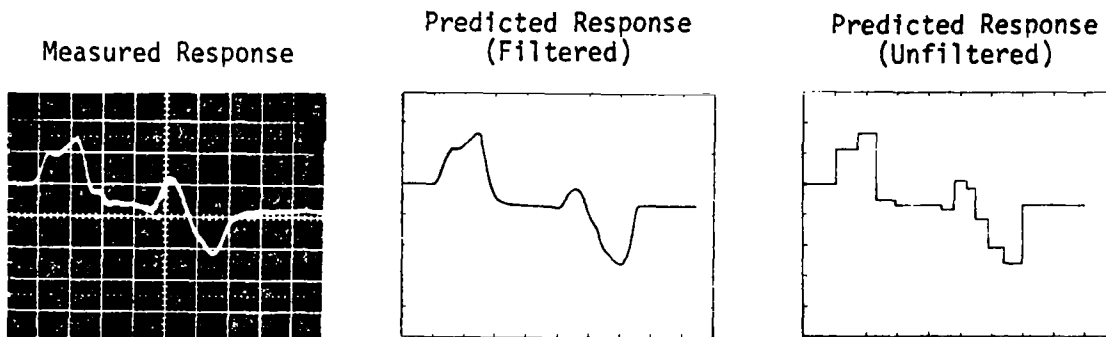


Figure 5. Voltage Waveform At the Load End of Wire-1 of Tube 2, with Wire 4 of Tube 1 Driven. Vertical Scale is 0.2 V/div; Horizontal Scale is 5 ns/div.

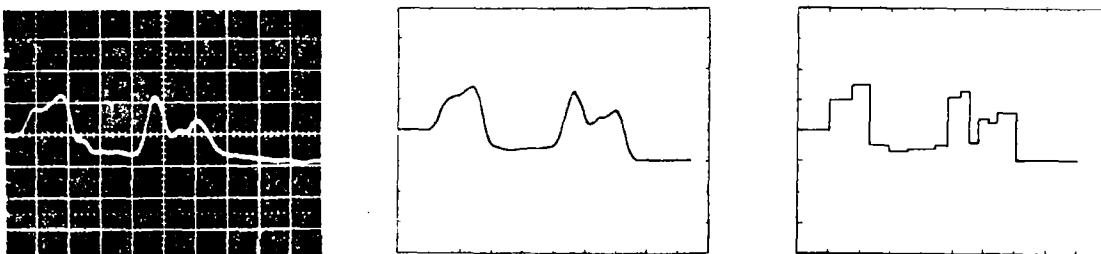
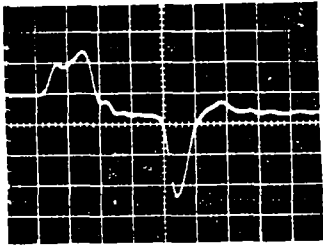
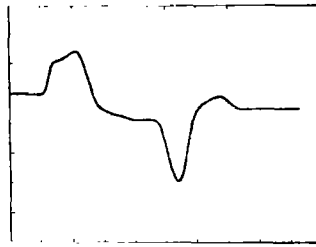


Figure 6. Voltage Waveform At the Load End of Wire-2 of Tube 2, with Wire 4 of Tube 1 Driven. Vertical Scale is 0.2 V/div; Horizontal Scale is 5 ns/div.

Measured Response



Predicted Response (Filtered)



Predicted Response (Unfiltered)

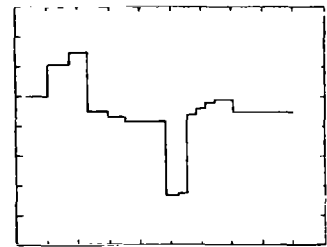


Figure 7. Voltage Waveform At the Load End of Wire 3 of Tube 2, with Wire 4 of Tube 1 Driven. Vertical Scale is 0.2 V/div; Horizontal Scale is 5 ns/div.

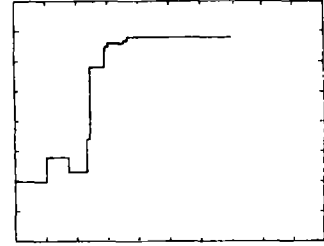
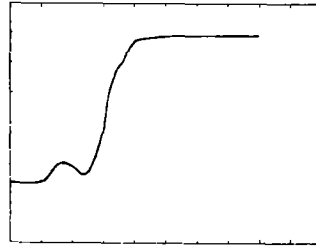
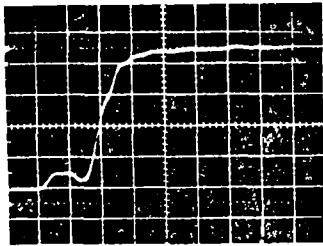


Figure 8. Voltage Waveform At the Load End of Wire 4 of Tube 3, with Wire 4 of Tube 1 Driven. Vertical Scale is 0.5 V/div; Horizontal Scale is 5 ns/div.

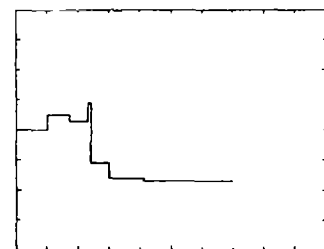
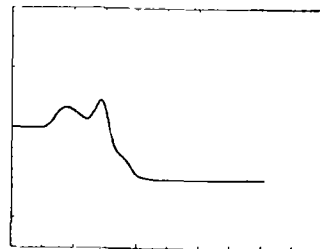
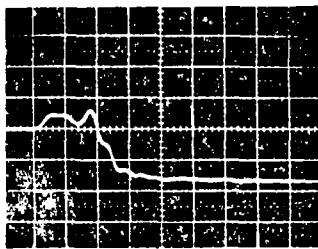
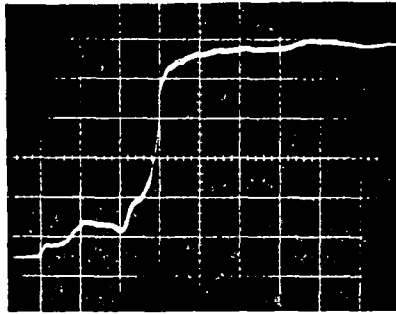


Figure 9. Voltage Waveform At the Load End of Wire 5 of Tube 3, with Wire 4 of Tube 1 Driven. Vertical Scale is 0.5 V/div; Horizontal Scale is 5 ns/div.

Measured Response



Predicted Response

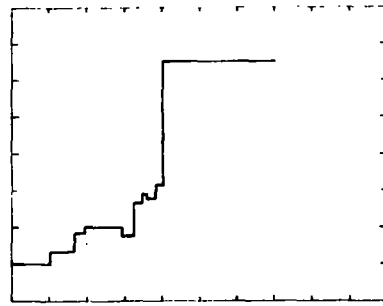


Figure 10. Voltage Waveform At the Load End of Wire 1 of Tube 1, with Wire 1 of Tube 2 Driven. Vertical Scale is 0.5 V/div; Horizontal Scale is 10 ns/div.

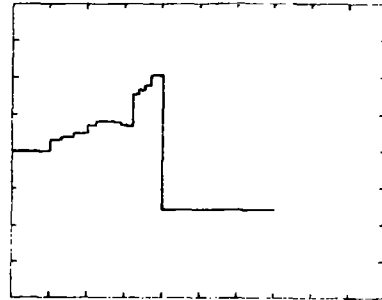
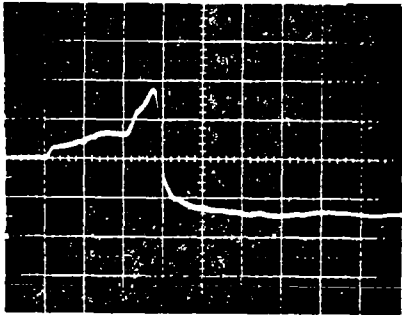


Figure 11. Voltage Waveform At the Load End of Wire 2 of Tube 1, with Wire 1 of Tube 2 Driven. Vertical Scale is 0.5 V/div; Horizontal Scale is 10 ns/div.

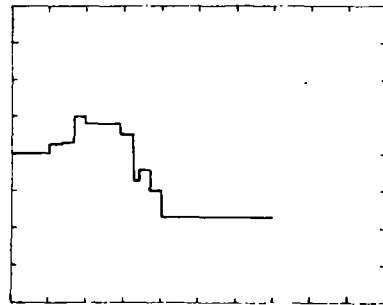
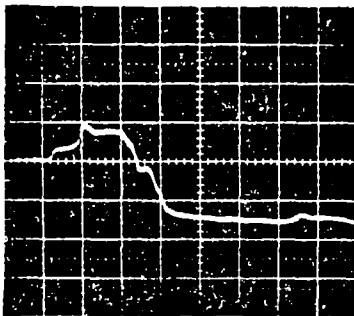


Figure 12. Voltage Waveform At the Load End of Wire 3 of Tube 1, with Wire 1 of Tube 2 Driven. Vertical Scale is 0.5 V/div; Horizontal Scale is 10 ns/div.

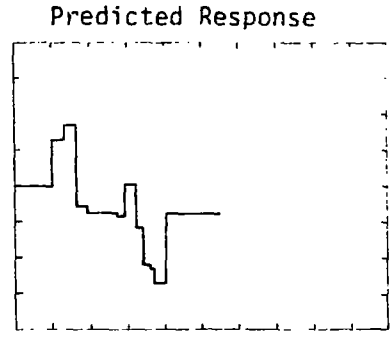
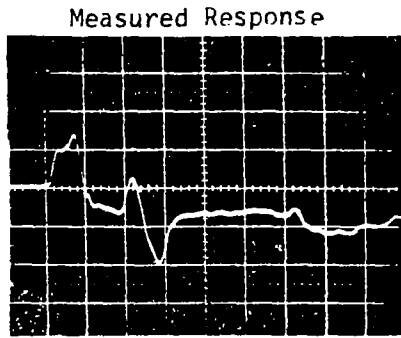


Figure 13. Voltage Waveform At the Load End of Wire 4 of Tube 1 with Wire 1 of Tube 2 Driven. Vertical Scale is 0.2 V/div; Horizontal Scale is 10 ns/div.

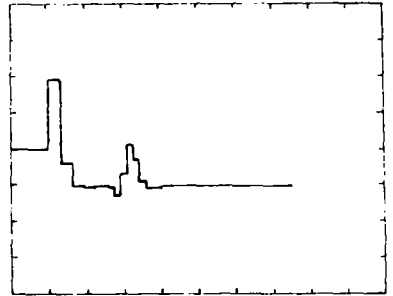
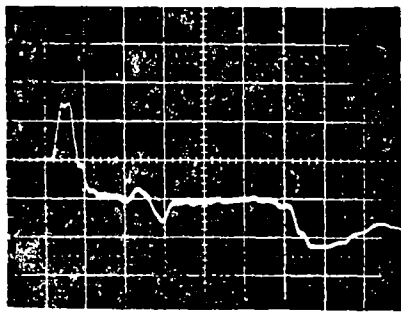


Figure 14. Voltage Waveform At the Load End of Wire 5 of Tube 1 with Wire 1 of Tube 2 Driven. Vertical Scale is 0.1 V/div; Horizontal Scale is 10 ns/div.

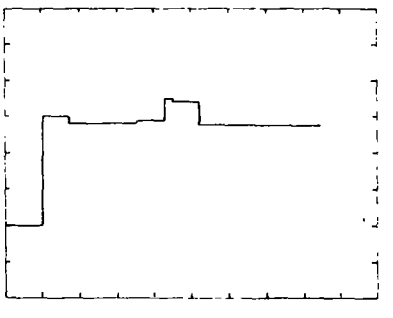
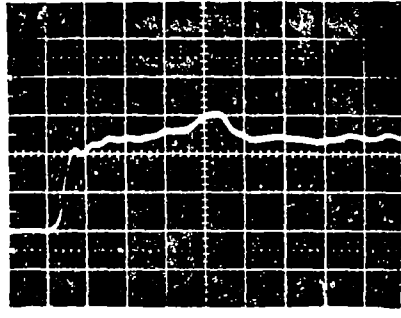
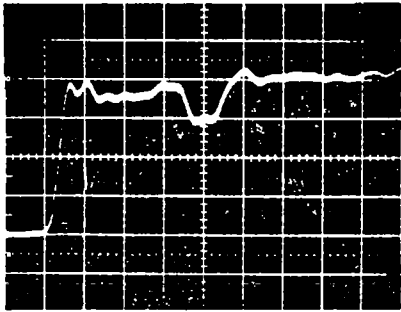


Figure 15. Voltage Waveform At the Load End of Wire 4 of Tube 3 with Wire 1 of Tube 2 Driven. Vertical Scale is 0.1 V/div; Horizontal Scale is 5 ns/div.

Measured Response



Predicted Response

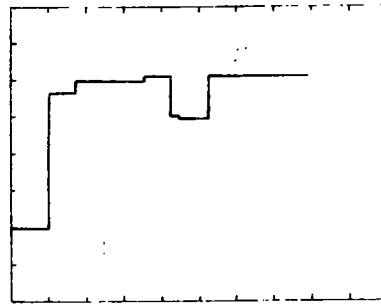


Figure 16. Voltage Waveform At the Load End of Wire 5 of Tube 3 with Wire 1 of Tube 2 Driven. Vertical Scale is 0.05 V/div; Horizontal Scale is 5 ns/div.

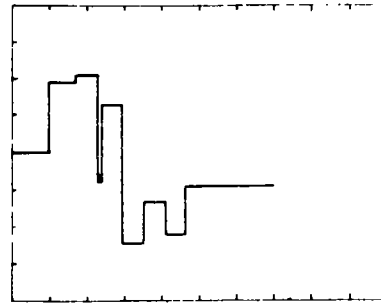
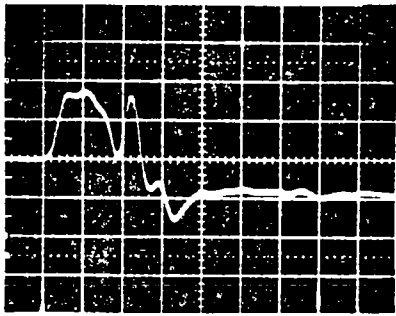


Figure 17. Voltage Waveform At the Load End of Wire 1 of Tube 1 with Wire 4 of Tube 3 Driven. Vertical Scale is 0.1 V/div; Horizontal Scale is 5 ns/div.

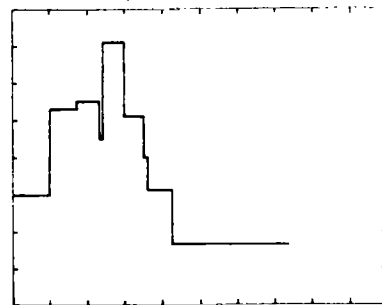
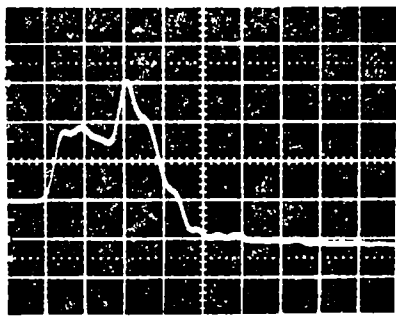
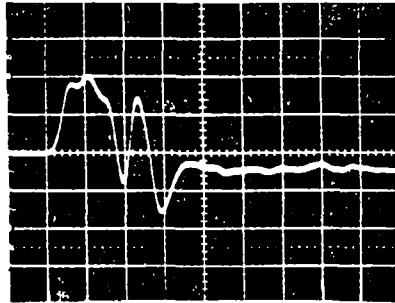


Figure 18. Voltage Waveform At the Load End of Wire 2 of Tube 1 with Wire 4 of Tube 3 Driven. Vertical Scale is 0.1 V/div; Horizontal Scale is 5 ns/div.

Measured Response



Predicted Response

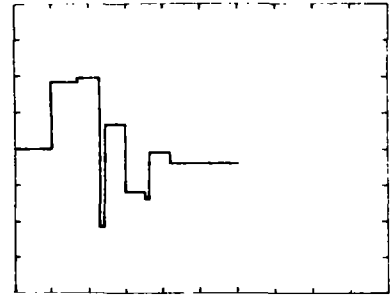


Figure 19. Voltage Waveform At the Load End of Wire 3 of Tube 1 with Wire 4 of Tube 3 Driven. Vertical Scale is 0.1 V/div; Horizontal Scale is 5 ns/div.

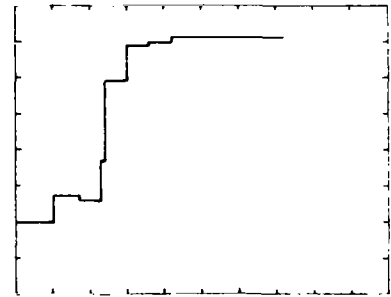
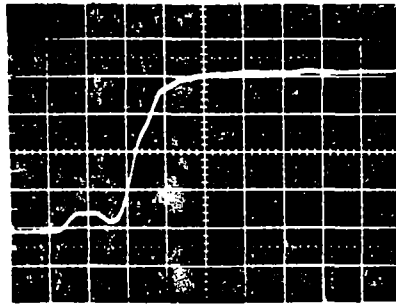


Figure 20. Voltage Waveform At the Load End of Wire 4 of Tube 1 with Wire 4 of Tube 3 Driven. Vertical Scale is 0.5 V/div; Horizontal Scale is 5 ns/div.

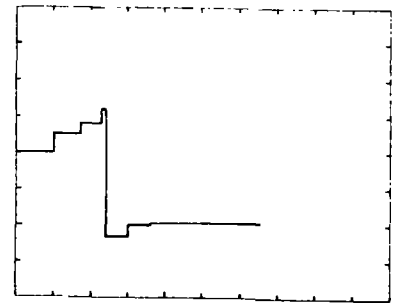
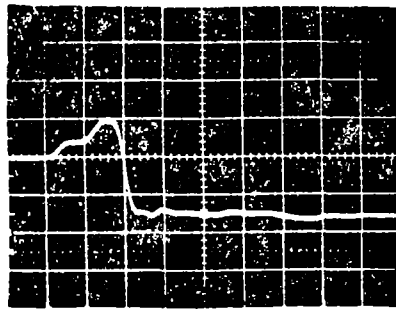
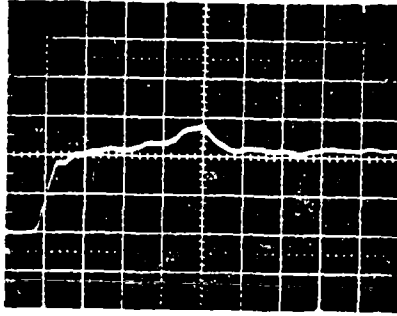


Figure 21. Voltage Waveform At the Load End of Wire 5 of Tube 1 with Wire 4 of Tube 3 Driven. Vertical Scale is 0.5 V/div; Horizontal Scale is 5 ns/div.

Measured Response



Predicted Response

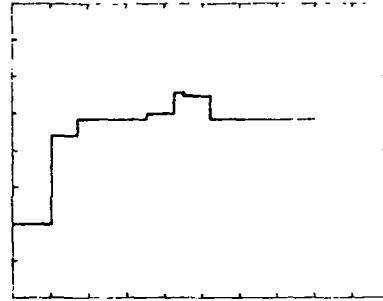


Figure 22. Voltage Waveform At the Load End of Wire 1 of Tube 2 with Wire 4 of Tube 3 Driven. Vertical Scale is 0.1 V/div; Horizontal Scale is 5 ns/div.

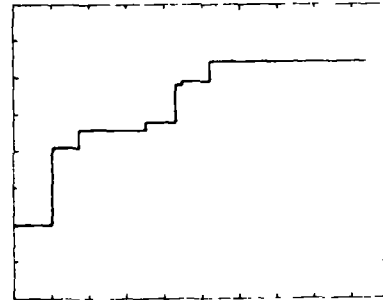
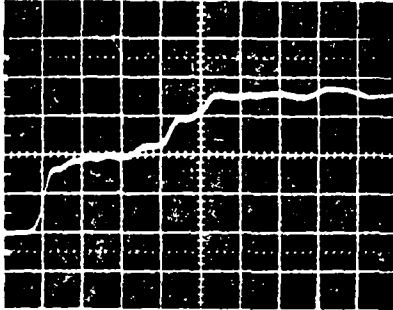


Figure 23. Voltage Waveform At the Load End of Wire 2 of Tube 2 with Wire 4 of Tube 3 Driven. Vertical Scale is 0.1 V/div; Horizontal Scale is 5 ns/div.

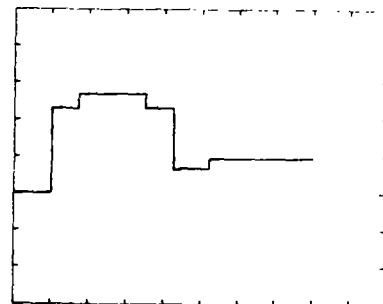
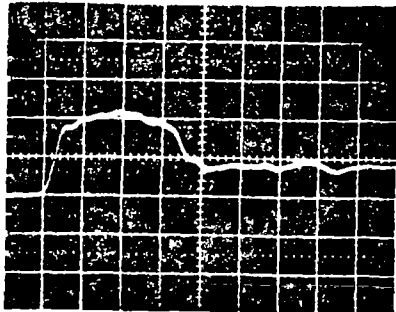



Figure 24. Voltage Waveform At the Load End of Wire 3 of Tube 2 with Wire 4 of Tube 3 Driven. Vertical Scale is 0.1 V/div; Horizontal Scale is 5 ns/div.



SECTION V
CONCLUDING REMARKS

A matrix analysis of lossless multiconductor branched lines with cross-sectionally inhomogeneous dielectrics has been presented. The theory provides a method of identifying all the modes excited in different branches of the line. This analysis in the time domain appears less involved than a similar frequency domain analysis and leads to a better conceptual understanding of the propagation modes.

The analysis given in this paper is applicable and can be applied to more complicated transmission lines having multiple junctions following the same step-by-step procedure.

REFERENCES

1. Electromagnetic Pulse Handbook for Missiles and Aircraft in Flight, Sandia Laboratories, EMP Interaction Note 1-1, September 1972.
2. Frankel, S., Cable and Multiconductor Transmission Line Analysis, Harry Diamond Labs. Washington, D.C., HDL-TR-091 June 1974.
3. Pipes, L. A., "Matrix Theory of Multiconductor Transmission Lines," Phil. Mag., Vol. 24, pp. 97-113, July 1937
4. Marx, K. D., "Propagation Modes, Equivalent Circuits, and Characteristic Terminations for Multiconductor Transmission Lines with Inhomogeneous Dielectrics," IEEE Trans. MTT, Vol. MTT-21, No. 7, July 1973.
5. Baum, C. E., T. K. Liu and F. M. Tesche, "On The General Analysis of Multiconductor Transmission Line Networks," AFWL EMP Interaction Notes to be published.
6. Baum, C. E., T. K. Kiu, F. M. Tesche and S. K. Chang, "Numerical Results for Multiconductor Transmission Line Networks," AFWL EMP Interaction Notes. Note 322, September 1977.
7. Paul, C. R., "On Uniform Multimode Transmission Lines," IEEE Trans. MTT, Vol. MTT-21, No. 8, pp. 556-558, August 1973.
8. Paul, C. R., "Useful Matrix Chain Parameter Identities for the Analysis of Multiconductor Transmission Lines," IEEE Trans. MTT, Vol. MTT-23, pp. 756-760, September 1975.
9. Paul, C. R., "Efficient Numerical Computation of the Frequency Response of Cables Illuminated by an Electromagnetic Field," IEEE Trans. MTT, Vol. MTT-22, No. 4, pp. 454-457, April 1974.
10. Amemiya, H., "Time Domain Analysis of Multiple Parallel Transmission Lines," RCA Review, pp. 241-276, June 1967.
11. Kunznetsov, P. I. and R. L. Stratonovich, The Propagation of Electromagnetic Waves in Multiconductor Transmission Lines. Oxford, England: Pergamon Press, 1964.
12. Chang, F. Y., "Transient Analysis of Lossless Coupled Transmission Lines in a Nonhomogeneous Dielectric Medium," IEEE Trans. MTT, Vol. MTT 18, No. 9, pp. 616-626, September 1970.

13. Krage, M. K. and G. I. Haddad, "Characteristics of Coupled Microstrip Transmission Lines With Inhomogeneous Dielectrics," IEEE Trans. MTT, Vol. MTT-21, No. 7, July 1973.
14. Schelkunoff, S. A., "Conversion of Maxwell's Equations Into Generalized Telegrapher's Equations," Bell System Technical Journal, Vol. 34, pp. 995-1043, September 1955.
15. Ramo, S., J. R. Whinnery and T. V. Duger, "Fields and Waves In Communication Electronics," John Wiley & Sons, Inc., New York, 1965.
16. Collin, R. E., Foundations for Microwave Engineering, McGraw Hill, New York, 1966.
17. Agrawal, A. K., K. M. Lee, L. D. Scott and H. M. Fowles, "Experimental Characterization of Multiconductor Transmission Lines in Frequency Domain," AFWL EMP Interaction Notes, Note 311, June 1977.
18. Agrawal, A. K., H. M. Fowles and L. D. Scott, "Experimental Characterization of Multiconductor Transmission Lines in Inhomogeneous Media Using Time Domain Techniques," AFWL EMP Interaction Notes, Note 332, February 1978.
19. Clements, J. C., C. R. Paul and A. T. Adams, "Computation of the Capacitance Matrix for Systems of Dielectric-Coated Cylindrical Conductors," IEEE Trans. EMC, Vol. EMC-17, No. 4, pp. 238-248, November 1975.
20. Paul, C. R. and A. E. Feather, "Computation of the Transmission Line Inductance and Capacitance Matrices from the Generalized Capacitance Matrix," IEEE Trans. EMC, Vol. EMC-18, No. 4, pp. 175-183, Nov. 1976.
21. Carey, V. L., T. R. Scott and W. T. Weeks, "Characterization of Multiple Parallel Transmission Lines Using Time Domain Reflectometry," IEEE Trans. IM, Vol. IM-18, No. 3, September 1969.